Experimental Modal Analysis of Appropriate Boundary Conditions for the Evaluation of Cross-Laminated Timber Panels for an In-Line Approach

Adam Faircloth Loic Brancheriau Hassan Karampour
Stephen So Henri Bailleres Chandan Kumar

Abstract

Transverse modal analysis of timber panels is a proven effective alternative method for approximating a material's elastic constants. Specific testing configurations, such as boundary conditions (BC) and location of sensor and impact, play a critical role in the accuracy of the results obtained from the experimental assessment. This article investigates signal-specific details, such as the signal quality factor, that directly relate to the damping properties and internal friction as well as frequency shifting obtained from six different BCs. A freely supported (FFFF), opposing minor sides (shorter length) simply supported, and major sides (longest length) free (SFSF), as well as the reverse of the SFSF configuration with minor sides free and major lengths simply supported (FSFS) and all sides simply supported (SSSS) setup, are investigated. Variations into the proposed methods used to achieve an FFFF supported system are also considered. A combination of experimental testing in parallel with finite element analysis was conducted to re-create the setup that would be used within a manufacturing facility for nondestructive assessment of full-size cross-laminated timber panels. The differences between all BC configurations for their resonance frequency quality and location indicate that a freely supported system provides higher-resolution results, good comparison of less than 10 percent error with the finite element analysis and experimental results, and advantages in a simple experimental setup for the intended application.

As mass timber construction becomes a more widely adopted and accepted building method for large-scale residential and commercial constructions (McGavin et al. 2020), the requirements for consistent and graded cross-laminated timber (CLT) panels from manufacturers are increasing, so a method is needed by which these panels can be rapidly evaluated (Steiger et al. 2010). Nondestructive evaluation (NDE) techniques are used as quick and effective methods for approximating the elastic properties of timber beams and boards with work toward a system for timber panel elements encroaching on a solution for in-line applications (Guan et al. 2017). An ideal solution to evaluate these panels would be a nondestructive grading system for CLT panels as they are produced from the manufacturing facility and thus a system designed around the application (Zhou et al. 2020). With the increased size and weight of these mass timber panels, the boundary conditions (BCs) used for NDE testing of these panels play a crucial role in their evaluation and need to be considered in full-size applications.

BCs directly affect the ability to acquire and observe the harmonic responses required to calculate mechanical properties (Damme et al. 2017). The dynamic response of these timber panels can contain reactions other than bending modes such as torsion and rigid body motion; based on the measurement method employed these bending modes will occur at smaller or greater amplitudes affecting the identification process (Zhou et al. 2017). Although completely free (FFFF) BCs are simple physically to set

The authors are, respectively, BEng, Queensland Dept. of Agric. and Fisheries, Salisbury Research Facility, Brisbane, Australia (Adam.Faircloth@daf.qld.gov.au [corresponding author]); PhD, CIRAD Centre for International Agric. Research and Development, Montpellier, France (loic.brancheriau@cirad.fr); PhD and PhD, School of Engineering and Built Environ., Griffith Univ., Gold Coast, Australia (h.karampour@griffith.edu.au, s.so@griffith.edu.au); PhD, Hyne Timber and Son, Brisbane, Australia (henri.bailleres@hyne.com.au); and PhD, Queensland Dept. of Agric. and Fisheries, Salisbury Research Facility, Brisbane, Australia (chandan.kumar@daf.qld.gov.au). This paper was received for publication in September 2020. Article no. 20-00062.

Forest Prod. J. 71(2):161–170.
doi:10.13073/FPJ-D-20-00062

up, there exists no analytical solution to BCs (Zhou et al. 2017). In contrast, a completely simply supported (SSSS) setup can be difficult to implement due to the constant contact requirements of the support conditions, although it has an exact analytical frequency equation. Maheri (2010) investigated the effects that several different BCs have on the damping of fiber-reinforced plastic panels and determined that for completely clamped (CCCC) and SSSS systems, the flexural frequencies obtained were higher, indicating a rise in the flexural stiffness of the measured panels and therefore resulting in a lower modal damping. Maheri (2010) states that the benefit of a SSSS system is based on the ability to determine the exact solution of modal plate vibrations; other BCs use approximation-based methods, such as the finite element method (FEM). However, experimental BCs cannot exactly simulate an FFFF or an SSSS response and in practice is commonly a combination of them. The presence of unwanted damping is more common in SSSS and CCCC configurations compared with FFFF; therefore, where damping is to be measured, an FFFF configuration would be most appropriate and can be realized easily.

Zhou et al. (2017) undertook a comparative study on four BCs proposed for the nondestructive assessment of wood-based panels within an in-line application and compared the elastic constant variations across the proposed BCs. Modal testing was conducted on panels 1.2 by 0.6 m with varying thickness for the four BCs, all sides free (FFFF), one side simply supported and the other three free (SFFF), one side clamped and the other three free (CFFF), and opposite parallel sides along minor strength direction (panel widths) simply supported and the remaining sides free (SFSF). During experimental testing, it was quickly realized that the support conditions required for an SFFF and CFFF system are not applicable to in-line use due to the physical difficulty in setting up the supports. It was concluded that all BCs are applicable for laboratory-scale experiments with the FFFF and SFSF configurations returning a 10 percent difference between static and NDE techniques used. Zhou et al. (2017) also noted that the nondestructive assessment of these panels was sensitive to the supporting conditions and setup of the experimental tests. Following up on this, Zhou et al. (2020) conducted a body of research aiming to quantify the bending and shear properties of CLT through modal analysis under an SFSF BC. Comparing experimental and theoretical results for the stiffness constants gave a 1.6 and 0.2 percent errors in major and minor axial directions, respectively, although a discrepancy was found between the experimental and theoretical shear moduli for the minor axial direction. This discrepancy is not unexpected due to the widths of the panel (minor dimension) being the simply supported dimension.

In a branch of the previous discussed study, Neiderwestberg et al. (2014) conducted a modal analysis on single layer CLT panels for BCs with the span parallel to the face grain direction and with the span perpendicular to the grain direction (SFSF and FSFS) as well as for the FFFF and SFFF systems. It was found that conducting these experiments was difficult to set up, as the simply supported conditions require constant contact being made between the supports and specimen surface. Neiderwestberg et al. (2014) compared the results from NDE testing of single-layer panels with the results from static tests for determining the elastic properties of the axial directions parallel (E_x) and perpendicular (E_y) to the face grain. The FFFF BC retuned errors of 1.0 and 18.6 percent difference for E_x and E_y, respectively. The SFFF system returned an acceptable error for E_x of –8.0 percent although the error for E_y was 40 percent. The SFSF condition produced the smallest average error of –3.5 percent for E_x and –3.7 percent for E_y. These results reinforce the argument that BCs have a direct effect of the accuracy in measuring key mechanical calculation descriptors, such as fundamental frequencies.

A comparative study conducted by Damme and Zemp (2018) found from the evaluation of bending wave dispersion curves in CLT that BCs dictated the acquisition of the resonant frequencies of tested beams. The results of the studies discussed above conclude that the conditions applied to restrict, suspend, or support the test specimen have a direct impact on the measuring accuracy of the experimental approach, therefore displaying the importance of an investigation into such methods. Neiderwestberg et al. (2014) and Zhou et al. (2017) did investigate the effect that BCs have on the comparison between static testing methods and the calculated elastic parameters, although validation through this method requires a large number of repeated experiments to be considered accurate. Concerning plate-like structures, the vibrational modes need to be considered in two dimensions and are a function of the sample density (kg/m^3) and the fundamental frequencies; therefore, changes in density and/or geometry are expected to have an effect on the material's behavior to vibrational excitation as well as fundamental frequency locations (Zhang et al. 2021).

The quality (Q) factor is a representation of the resonant frequency peak resolution; nondestructive assessment of timber elements relates to specific material properties and natural frequencies of the measured samples, so it is important to ensure that the frequencies used for this assessment are clearly defined in the frequency spectrum (Shirmohammadi et al. 2020). These descriptors are commonly used for the evaluation of acoustics and sound properties of materials where BCs remain consistent and material properties are evaluated (Labonnote et al. 2013). This study aimed to fix the material (CLT) and evaluate a number of BCs; rather than characterizing the material through the NDE method applied with BCs, the supporting conditions will be evaluated to determine their suitability. From the above, it is the conclusion of the research team that there is a noticeable gap in relating BCs to the intended application of an in-line evaluation system for CLT panels as well as assessing the effects that each BC has on accurately measuring the vibratory response of these panels. Therefore, the objective of this study was to investigate a number of BCs as selected based on previously conducted and relevant research and determine a best-suited BC for application to an in-line NDE system for assessing the elastic constants of CLT panels.

Materials and Methods

Test specimens

The samples used for assessment were CLT panels comprised of three layers, with each proceeding layer perpendicular to the last. The panels were 3.2 by 2.8 by 0.075 m in size made up of radiata pine (*Pinus radiata*) with

an average density of 475 kg/m^3 measured from the test specimens. As introduced by Zhang et al. (2021), the density and corresponding geometrical properties will affect the frequency locations; therefore, to limit the number of variables within the study, a single species type and grade of CLT were selected. The geometric properties, density, and estimated elastic constants were kept consistent for the FEA. The major stiffness properties of wood are related to the axial direction parallel to the grain (Steiger et al. 2010), so the major axial direction is recorded as the direction parallel to the face board layer orientation (L_x), and the minor axial direction is considered as perpendicular to the face board orientation (L_y). CLT is comprised of laminated boards bonded to each surface, although the edges between adjacent boards are not bonded. One assumption made in this study is that the discontinuities between adjacent boards are negligible to the stress wave propagation and that the CLT panels can be modeled as a single plate (Steiger et al. 2010).

Experimental protocol

BCs selected for the study were achieved by using a range of readily available products and materials that would be applicable to an in-line manufacturing scenario, as is the intended purpose of the system. The SSSS system was achieved by using a simple timber border of a 50-mm width around the perimeter of the panel (Fig. 1a); this was the most practical and achievable arrangement to ensure a sturdy setup and minimal contact with the panel. Due to the simplicity in the setup requirements, this BC may be attractive to industry; it is important to ensure that all edges are making contact with the boards, or BCs will not be accurately simulated. The SFSF and FSFS BCs were constructed using raised supports (Fig. 1b) placed as close to the edges as practical where support was required. This configuration was also simple in its setup, as workers were able to lift the panels into place with ease. It was found equally important with this setup to ensure that the SS edges were in constant contact with the supports so as not to introduce errors. These configurations are presented in Figure 1. To investigate the most effective and practical setup, three configurations of a freely supported system were selected and are also depicted in Figure 1. The three configurations consist of airbag supports (FFFF-1) underneath the panel at four points (Fig. 1c), nylon recovery straps to suspend the panel flatwise (FFFF-2) at four points (Fig. 1d), and nylon straps attached to the edge of the panel to suspend it edgewise (FFFF-3) at two points (Fig. 1e). Each of the six BCs was investigated using the setups shown in Figures 3 and 4 with findings discussed through this article. The adopted configurations of an SFSF BC consist of two parallel sides of the panel supported. The placement of the supports and width of the contact area have been arranged so that Figure 1a the simply supported (SS) sides are supported as close to the edge as practical (Fig. 1a) and the contacting area is minimal (Fig. 1b); two scenarios are investigated where the major axial lengths are SS (3.2-m length) and where the minor lengths are SS (2.8-m length). Further details on the physical setups required for each of the BCs are depicted in Figure 1 (see also Fig. 2).

Vibration assessment

A typical modal testing setup was employed for assessment of BC configurations to determine the vibrational characteristics of the testing setup. As shown in Figure 3, the panel is excited by an impacting hammer (IEPE Brüel & Kjær type 8206 impact hammer) on the surface of the panel; this impulse is then measured through a surface-mounted accelerometer (BCP Piezoelectronics model 352C33 single-axis accelerometer) affixed to the panel. The impulse propagates through the panel, as indicated by the curved lines in the figure, where the response is collected by the accelerometer.

The raw signal obtained from the impact hammer and accelerometer is then processed through the LabVIEW-based programming environment with a sound and vibration

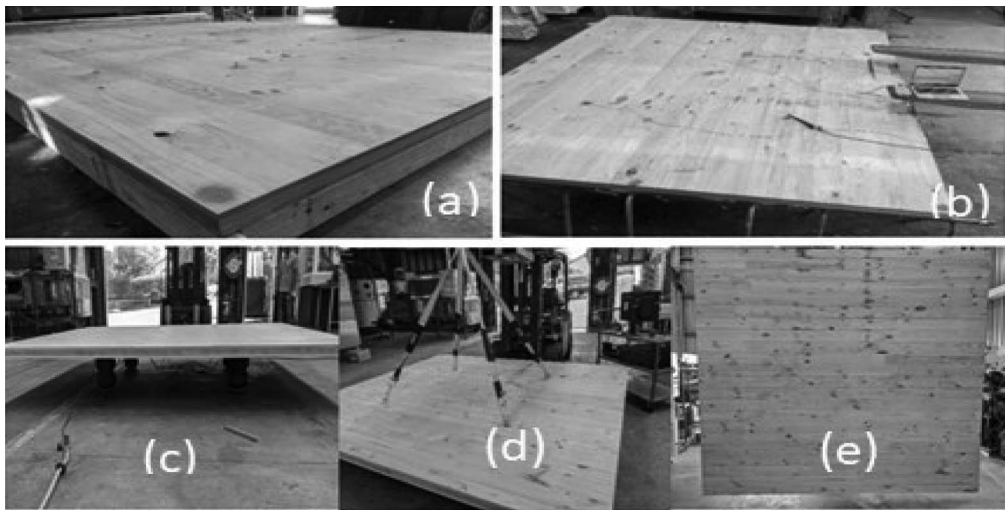

Figure 1.—Experimental setup of (a) SSSS, (b) SFSF (shown) and FSFS BCs, (c) airbags (FFFF), (d) suspended on flat (FFFF), and (e) suspended on edge (FFFF). SSSS = all sides simply supported; SFSF = major sides (longest length) free; FSFS = minor sides free and major lengths simply supported; BC = boundary condition; FFFF = all sides freely supported.

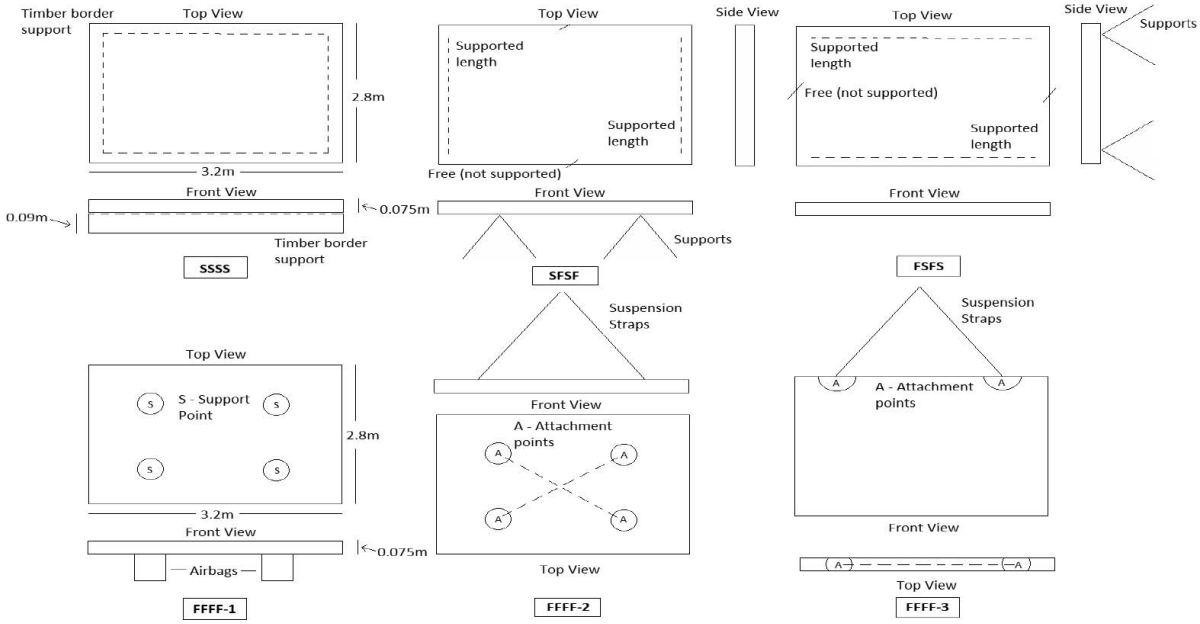

Figure 2.—Diagram of the boundary conditions shown in (a) through (e).

card (National Instruments Sound and Vibration Module NI 9234 24-bit ADC) where the signal is sampled at a rate of 8 kHz, for a total 51,200 samples acquired, giving a sampling resolution of 0.156 Hz, for an acquisition duration of 6.4 seconds. The deconvolution equation is defined below by determining the result of $y(n)$ of the following convolution formula:

$$y(n) = \sum_{k=0}^{N_h-1} h(k) \times x(n-k) \tag{1}$$

where $x(k)$ is the input (impact hammer) signal, $h(k)$ is the output (accelerometer) signal, and $y(n)$ is the convolved response. Assessment of the signal quality is conducted on the FRF output; the response was generated with no additional post-processing techniques, such as windowing to assess raw data response. The formulas presented in Equations 2 and 3 show the process of assessment used for determining the resonant peak resolution:

$$Q = \frac{f_R}{f_2 - f_1} \tag{2}$$

$$\text{location of } f_{1,2} = \pm \frac{A_{\max}}{\sqrt{2}} \tag{3}$$

where Q is the quality factor determined by the natural frequency, f_R, divided by the difference between the upper and lower peak frequency boundaries, f_2 and f_1, respectively, and $A_{\max}$ refers to the amplitude of the natural frequency, f_R (Spromann et al. 2017). Prior to experimental testing of the selected BCs, FEM modeling was conducted to model modal responses of a three-dimensional plate to determine locations on the panel that experience minimum and

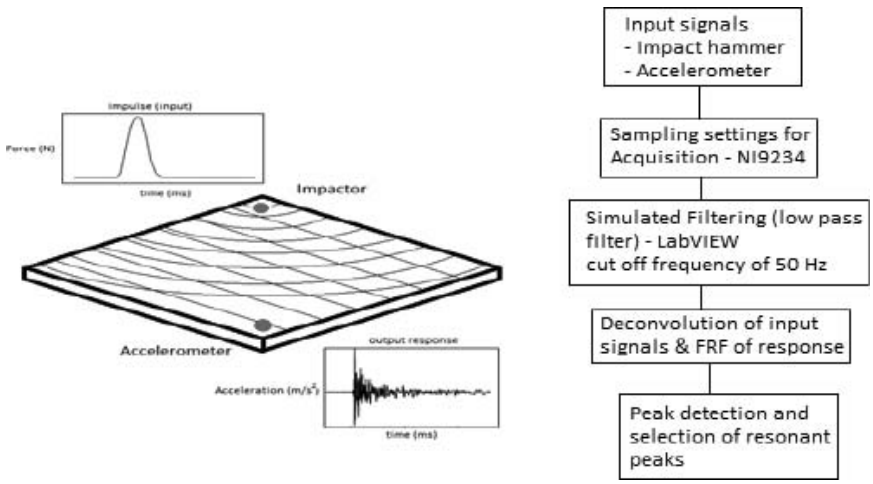

Figure 3.—Impulse location and stress wave propagation through a cross-laminated timber panel.

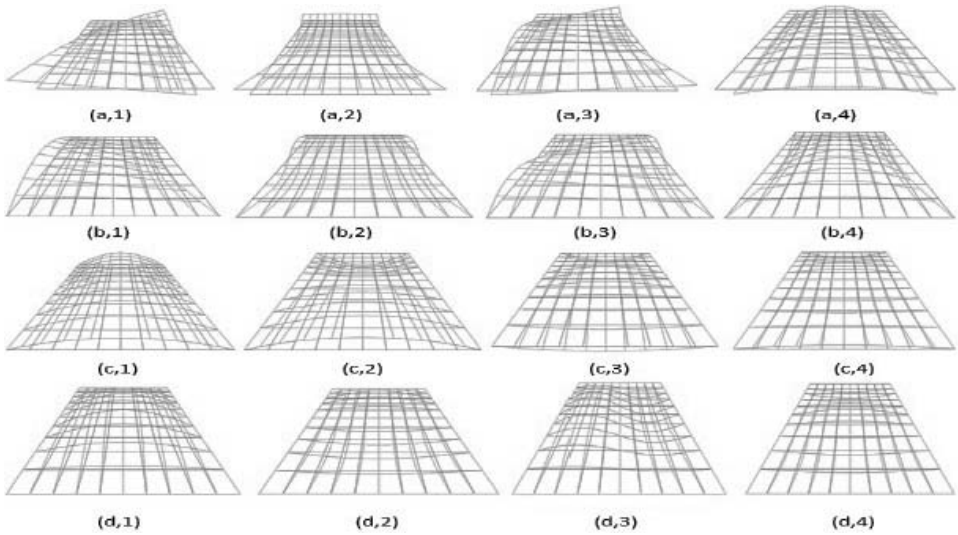

Figure 4.—First four mode shapes for the four boundary conditions: (a) FFFF, (b) SFSF, (c) FSFS, and (d) SSSS. FFFF = all sides freely supported; SFSF = major sides (longest length) free; FSFS = minor sides free and major lengths simply supported; SSSS = all sides simply supported.

maximum deflections to ensure that the support locations for FFFF conditions will not obstruct the modal response. Guan et al. (2017) began with a similar approach by modeling the response of a panel under free supporting conditions to determine appropriate locations for the nodal supports. The areas that experience minimal deflection, referred to as nodal points, are the support locations and areas of maximum deflection, referred to as antinodes, the impact and sensor locations; by observing up to four mode shapes, as seen in Figure 4, the best-suited locations for supports were determined. This modeling was undertaken for all BCs to determine appropriate impacting and sensing locations as well as support points for the FFFF configuration. Figure 4 shows the first several modes obtained through theoretical modeling of a thin, orthotropic plate with dimensions, density, and BCs the same as those of the CLT panels assessed in this study. It can be seen in the four BC setup areas of maximum deflection and minimal movement.

Finite element analysis

Modeling conducted to obtain the following modal responses was done through the software platform Cast3M. A three-dimensional, solid rectangular plate was used to simulate the CLT panel with the same geometrical parameters as those defined in the test specimen section. The assumption that CLT acts as a solid plate follows the trend of previous literature where non-edge bonding has a negligible effect on the results due to there being little loss in mass from this difference and that the added air gaps between boards would affect not the frequency location but rather the amplitude of the peaks. Poisson's ratio of material properties has been set to 0.3, as regularly used for the theoretical analysis of common pine species (Santoni et al. 2017). Elastic parameter estimations were set on the basis of the information provided by the manufacturer of the CLT panels.

The mode shapes above show that at ¼ distances from the corners of the panel, there appears to be minimal movement, although it is visible in modes 2 and 4. Similarly, the corners of the panel experience maximum deflection, which is expected with the FFFF BCs. The modes in Figures 4b through 4d show the panel's response with either two opposing or all sides SS. Looking at the responses from these three configurations, it can be seen that at ¼ distances from the corners of the panel, deflections can be measured for the majority of modes, contradictory to the observed response for Figure 4a. The results of the FEM modeling leads to the experimental test setup for each BC as depicted in Figures 2 and 5, containing support, impact, and sensor locations.

Results and Discussion

The tests consisted of six BC variations and the accuracy of the signal in obtaining the maximum number of modes. Theoretical simulations of thin orthotropic plates were conducted as displayed in Figure 4 using Young's moduli estimations of 10 GPa for the major direction (E_x) and 1.5 GPa for the minor direction (E_y) determined from the design properties of the CLT panels and the assumption that Young's modulus along the grain direction is $\geq$10 times that measured perpendicular to the grain direction (Damme and Zemp 2018). Shear moduli estimations of 0.8 GPa for G_{xy}, and 2 GPa for G_{yz} and G_{xz}, respectively, were used based on the design properties of the CLT. From these results for the selected BCs, it was found that the first 12 mode shapes fit within the frequency range of 10 to 200 Hz with frequencies lower than 10 Hz producing the rigid body motion (RBM) of the system. Zhou et al. (2017) found that to accurately approximate the elastic constants of timber composite panels, it is ideal to acquire 10 to 15 modes; therefore, based on these findings and the results of the theoretical component, a minimum of 12 modes were targeted for all BC investigations. Figure 5 shows the overlaid responses from the six BCs. Figure 6 (top plot) shows the variation within the FFFF BCs. Although the frequencies appear within a consistent range of each other, a shift in the frequencies for all modes is observed; these results are from tests conducted with a single panel to minimize introduced variations. It can also be found that BCs affect the amplitude of the FRF, which can impact resonance detection and signal quality. The bottom plot contains the SFSF, FSFS, and SSSS BC responses; both SFSF and FSFS responses appear to contain resonant frequencies within the range of

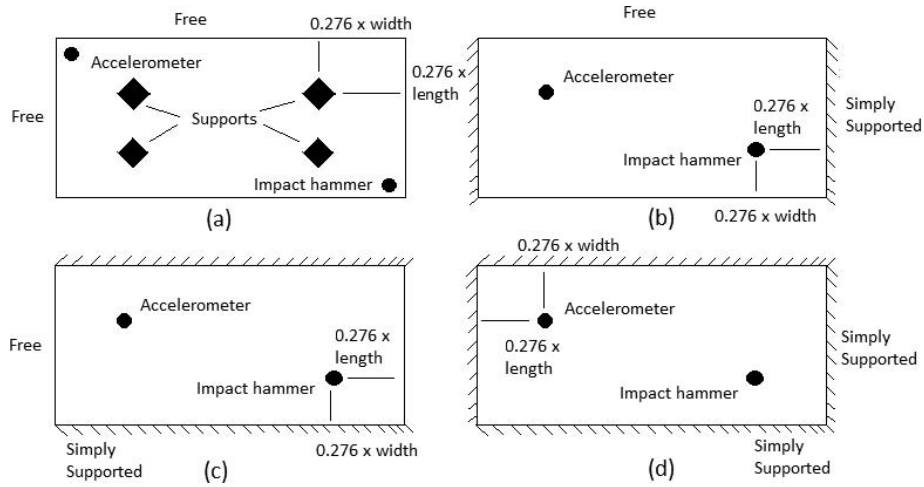

Figure 5.—BC supports and recommended impact locations: (a) FFFF, (b) SFSF, (c) FSFS, and (d) SSSS. BC = boundary condition; FFFF = all sides freely supported; SFSF = major sides (longest length) free; FSFS = minor sides free and major lengths simply supported; SSSS = all sides simply supported.

each other with some minor shifting present. Differences between SFSF and FSFS are expected due to the change in configuration, as panel dimensions of length and width do not differ greatly from each another. The FRF in Figure 6 (bottom plot) for SSSS is more clear and more resolvable, allowing for confident peak detection.

Figure 6 contains torsional modes and bending modes along both major and minor directions; for the modal determination process proposed in this study, bending modes in both major and minor directions will be more pronounced, although all are viewed in the spectrum shown in Figure 6. The location of resonant frequencies can be obstructed by the overlap of some modes, noted as double peaks in Zhou et al. (2017); this is due to the proximity of the resonance modes coupled with a high damping ratio. This occurrence is validated through successful comparison of the experimental data and detected resonant peaks with the theoretical simulated modal frequencies presented in Figure 7 showing the comparative error. Comparing the identified resonant frequencies with the corresponding mode shape frequencies acquired from the theoretical analysis will determine the effect that the frequency shift has on identifying the correct modes as well as determining the most appropriate BC that matches with the theoretical response. Figure 7 represents the error percentage comparison for each of the six BCs against their respective simulated response for a panel comprised of

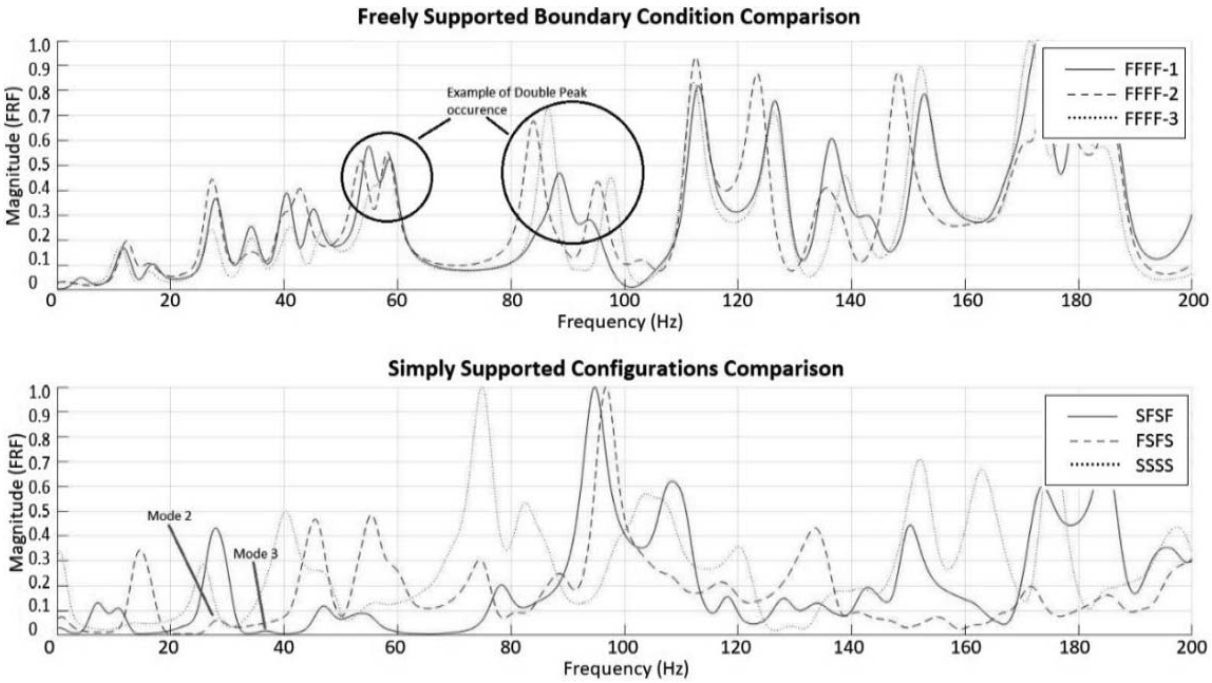

Figure 6.—FFFF variation comparison; SFSF, FSFS, and SSSS comparison (bottom). FFFF = all sides freely supported; SFSF = major sides (longest length) free; FSFS = minor sides free and major lengths simply supported; SSSS = all sides simply supported.

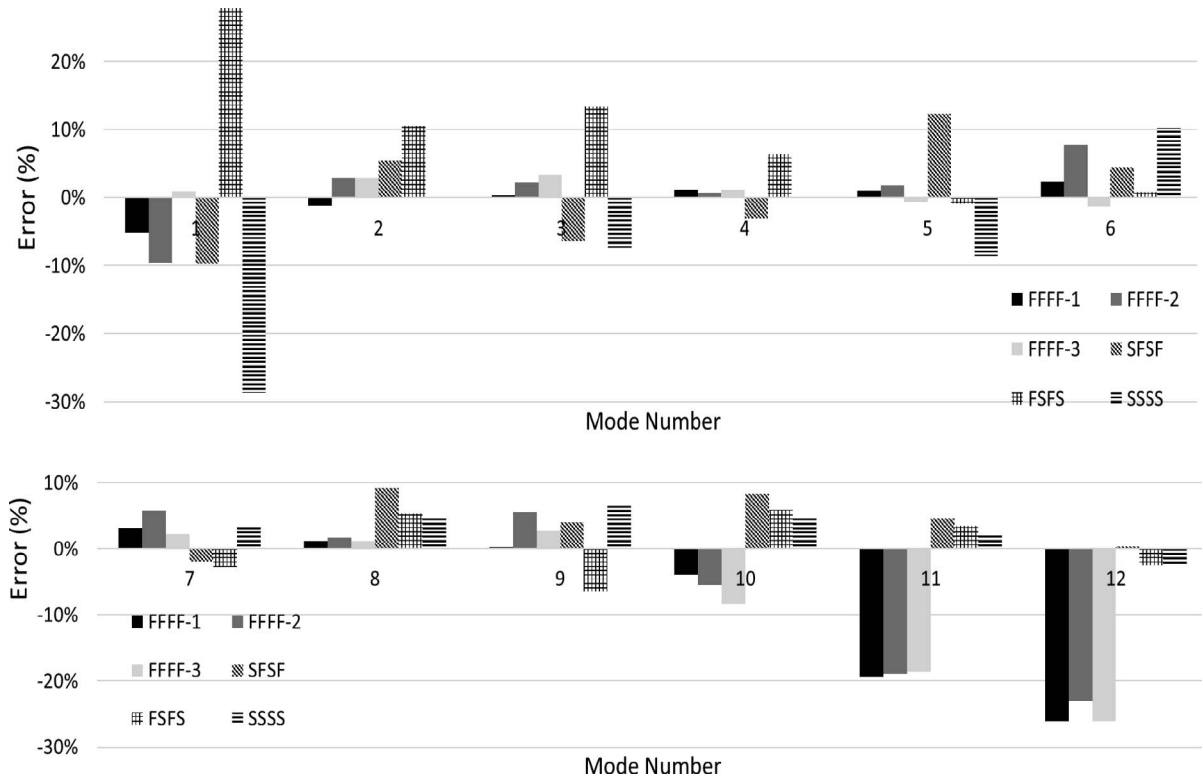

Figure 7.—Comparative results between simulation and experimental resonance frequencies for the six boundary conditions: modes 1 to 6 (top) and modes 7 to 12 (bottom).

the same physical properties (dimensions, density, and BCs). The results presented in Figure 7 show that as the frequency increases, so does the error for the three FFFF BCs with the FFFF-1 configuration being able to measure up to the 10th mode with a maximum variation in results of ±5 percent.

While all FFFF conditions produced similar comparative results, the error varies with each configuration with FFFF-1 producing the lowest error percentage, followed by FFFF-3, and FFFF-2 with the highest error of the three. The SFSF BC has a considerable error for lower modes, most likely due to possible discrepancies in the BC setup. SFSF's third mode was recorded, although as it was difficult to detect due to low amplitude; this, in combination with the error between frequencies, could indicate an error in the physical setup. Observing Figure 6 (bottom) of the experimental response from the FRF below 50 Hz, instances of expected modes with low amplitude have been highlighted for mode 2 of FSFS and mode 3 of SFSF. From the modal responses displayed in Figure 3, mode 3 is a torsional mode, which could be another contributor to the low amplitude measured. The FSFS BC returns a similar error percentage to SFSF from modes 1 to 4 and, as shown in Figure 6 (bottom plot), has a low amplitude, making it difficult to detect. It can also be noted from FSFS that resonant frequencies above 100 Hz start to decay in resolution and amplitude. The SSSS BC shows high error from modes 1 to 3, although it is able to accurately identify modal frequencies with errors below ±10 percent for modes 4 to 12.

Comparing these results with signal Q factors provides a better understanding of the effects that each of the nominated BCs are having on the experimental evaluation. Using Equations 2 and 3, the Q factors were determined and are presented in Figure 8, displaying the six BCs and their mean and range to the calculated Q factors. These values show that a high quality factor will correspond to a clearly defined peak due to the calculation method; therefore, BCs that obtain consistent and high Q factors are ideal for peak detection. This assumption is proven correct in Figure 8 with the FFFF displaying higher Q factors than SFSF, FSFS, and SSSS, as expected. The Q factor plot indicates that for the three FFFF configurations, the FFFF-2 produces the highest average Q factor, although the average difference between FFFF-2 and FFFF-1 is small with FFFF-1 having a smaller variation. This can be further reinforced by comparing the quality of the signals with the comparative data displayed in Figure 7. SFSF, FSFS, and SSSS have Q factors in the similar range as each other with FSFS having the lowest Q factor average. SSSS has a similar average but a larger range of values; SFSF returned a higher average but a large variation in results. From these results, it can be concluded that the three FFFF BCs provide clear results, and the setup developed through this study is repeatable, established from the consistent Q factors. Of the three FFFF configurations, FFFF-1 produced a consistent Q factor in comparison to the other five configurations tested. Additionally supports used for FFFF-1 are simple to operate, allowing for rapid setup and testing, as well as being able to support a wide range of weights from 300 kg to several tonnes, allowing for various sample sizes and weight to be assessed. Testing with FFFF-1 was conducted using an inflation pressure of 180 kPa based on manufacturer recommendations; as part of this study, a sensitivity assessment of the pressure used for FFFF-1 corresponding to the dynamic assessment of the CLT panels was conducted. For FFFF-1 tests, pressure variations from 70 to 700 kPa in increments of 70 kPa were conducted; Figure 9 presents the comparative data from these sensitivity tests.

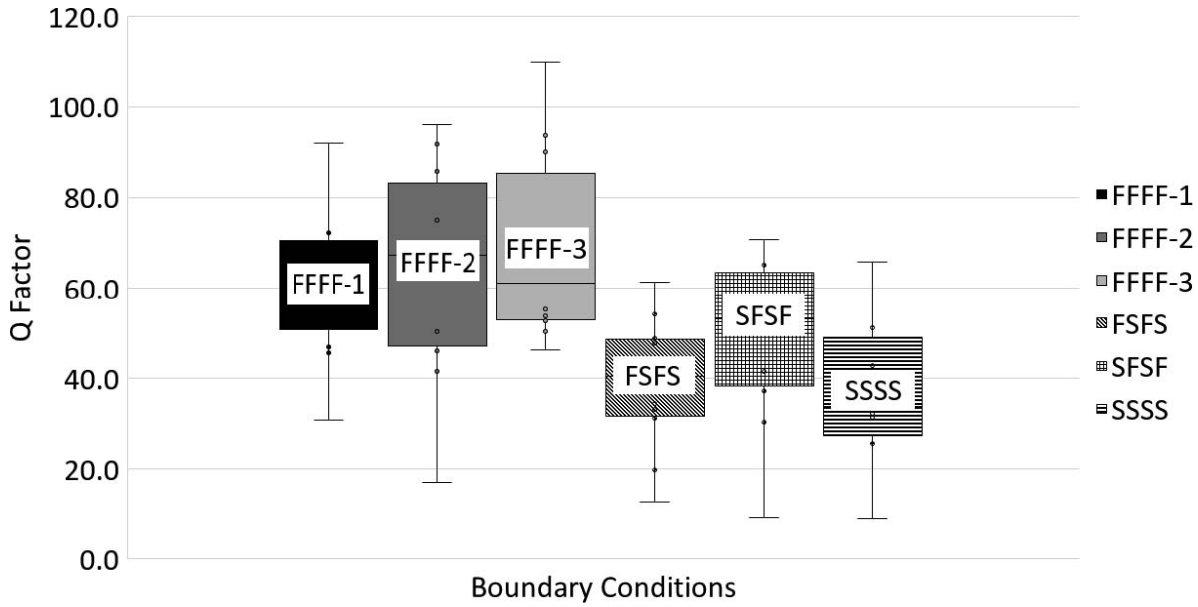

Figure 8.—Quality factor for tested boundary conditions.

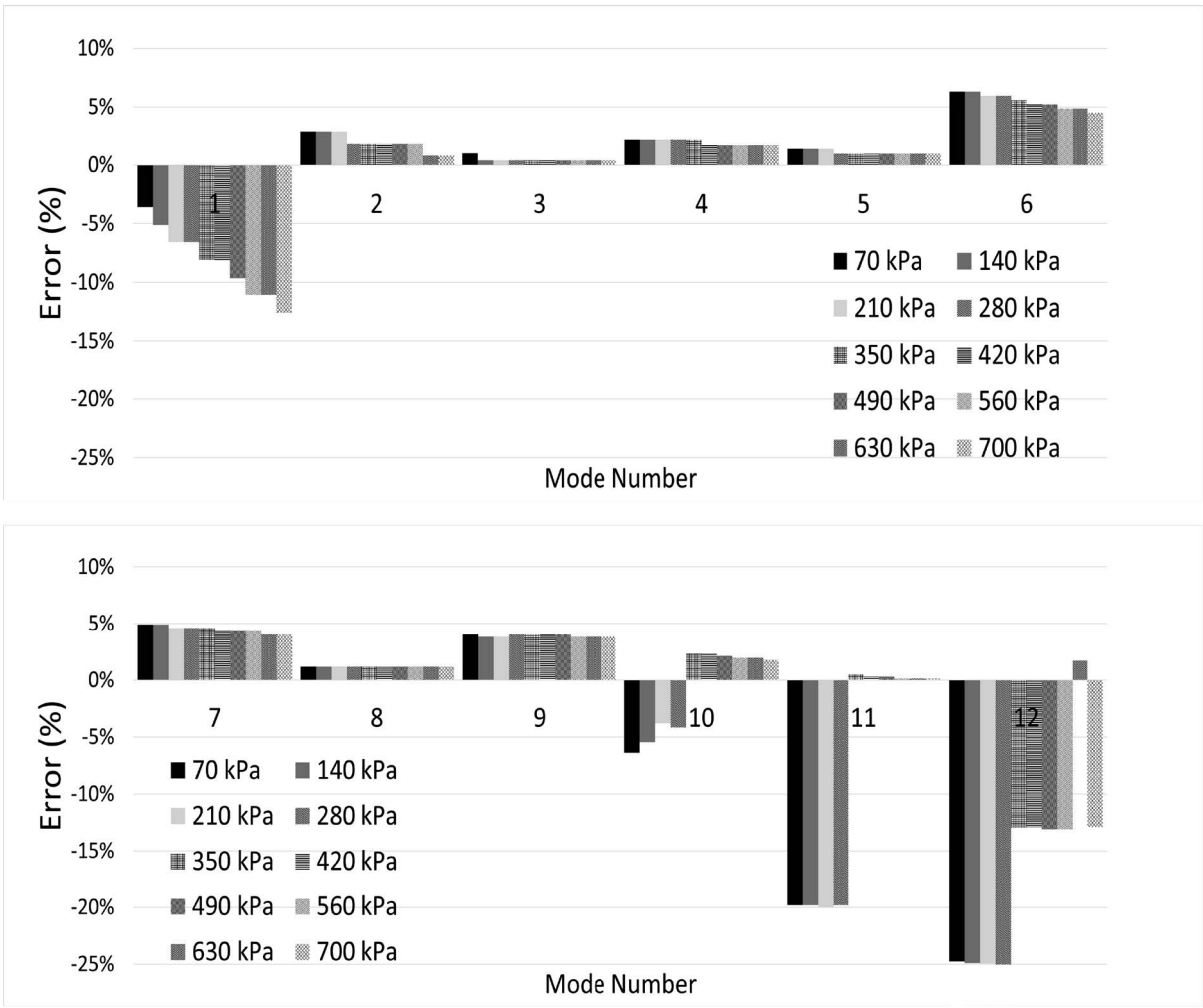

Figure 9.—Comparative results for airbag pressure investigation: modes 1 to 6 (top) and modes 7 to 12 (bottom).

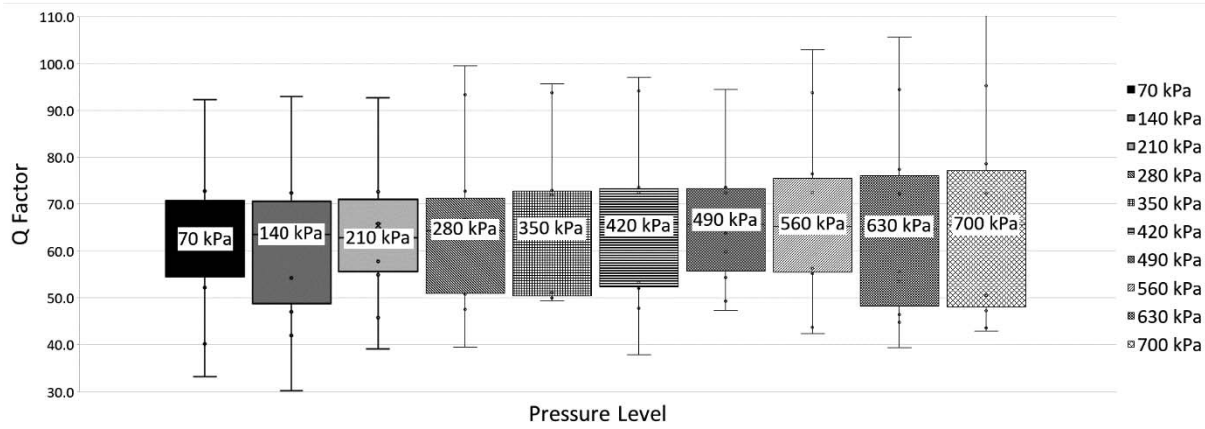

Figure 10.—Pressure sensitivity investigation: changes in signal quality with rising pressure.

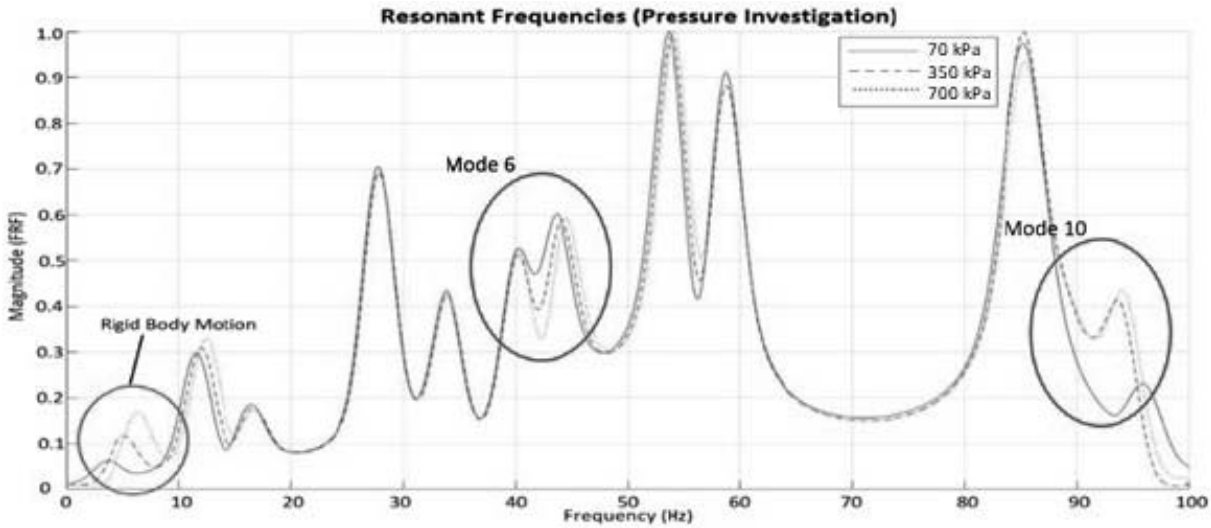

Figure 11.—Rapid decrease in peak quality, leading to unwanted error in peak identification (presented in 70, 350, and 700 kPa).

Figure 9 shows that with increasing pressure, the error between simulated and experimental increases slowly over the incremental tests. As the pressure increases, the resonant frequency positions shift higher with some frequencies decreasing in amplitude (beginning to dampen); this effect shows the transition from a freely supported node to a simply supported node. The inflation pressure affects the panel's ability to respond and propagate vibrations when excited by an impact; for industry to achieve as close to a freely supported system as practical, the optimal pressure used to obtain the maximum number of modes with minimal error is crucial to the system. The physical setup for an FFFF system refers to the supporting conditions having a negligible effect on the observed resonance frequencies, that is, allowing for undampened vibrations to be observed. The RBM varies from 3.506 to 6.17 Hz and from 70 to 700 kPa, respectively; the amplitude also increases, as shown in Figure 11. This change in RBM properties, especially amplitude, can cause errors during peak identification and should be noted to ensure that frequencies of this range are neglected. Comparing 70, 350, and 700 kPa, it can be seen in Figure 11 that modes 6 and 10 decrease in amplitude and quality as the pressure increases. From these findings of frequency shifting and amplitude decrease, it is concluded that the supports reach a point where the pressure supplied causes the supports to become stiffer, allowing for less vibratory movement and damping some modal responses, thus causing the supports to act less as free support conditions and more as simply supported configurations at those points. Figure 10 shows the change in Q factor with the increasing pressure. The Q factor results show that as the pressure increases, the range of the measurements decreases up to 350 kPa and then begins to increase again. The average Q factor value is consistent, although due to the variations in range, the error is lowest for pressure measurements from 70 to 210 kPa between modes 1 and 5, as shown in Figure 9.

Conclusions

Six BCs identified in this article are suitable applications for an NDE system for CLT panels, and a freely supported system was identified as being the most repeatable configuration providing consistent quality factors, a good comparison of $<\pm 8\%$ error between theoretical and simulated modal frequency, and a simple setup for manufacturers to implement in-line. Of the three FFFF

variations assessed, FFFF-1 returned clear and easy-to-interpret results as well as being a robust and repeatable configuration. Average error between modes 1 to 10 was $<\pm 5$ percent. Based on the results of the sensitivity analysis conducted on the pressure used to inflate the airbags used for FFFF-1, the optimal pressure range was >70 to and <210 kPa; a pressure of 180 kPa was selected for the comparative BC tests. By considering not only the accuracy and performance of the BC but also the application to industry, this study outlines FFFF-1 as a more suitable configuration for NDE testing of CLT panels in an in-line environment. The BC allows for rapid, safer, and effective assessment of the material to a large scale while being of suitable difficulty to prepare and set up with little equipment needed (airbags, accelerometer, DAQ, and signal acquisition software); the FFFF-1 BC configuration with a pressure of 70 to 210 kPa was found to accurately represent an FEA model of a freely supported BC. Assumptions made during this study have been the effects of modeling the CLT panel as a solid plate element and not the accumulation of the individual boards (edge bonding effects not taken into account).

Literature Cited

Damme, B. V., S. Schoenwald, and A. Zemp. 2017. Modeling the bending vibration of cross-laminated timber beams. *Eur. J. Wood Wood Prod*. DOI:10.1007/s00107-016-1152-9

Damme, B. V. and A. Zemp. 2018. Measuring dispersion curves for bending waves in beams: A comparison of spatial Fourier transform and inhomogeneous wave correlation. *Acta Acustica United Acustica* 104(2):228–234.

Guan, C., H. Zhang, X. Wang, H. Miao, L. Zhou, and F. Liu. 2017. Experimental and theoretical modal analysis of full-sized wood composite panels supported on four nodes. *Materials* 10(6): 1–15.

Labonnote, N., A. Ronnquist, and K. A. Malo. 2013. Semi-analytical prediction and experimental evaluation of material damping in wood panels. *Holzforschung* 67(3):333–343. DOI:10.1515/hf-2012-0095

Maheri, M. R. 2010. The effects of layup and boundary conditions on the modal damping of FRP composite panels. *Journal of Composite Materials*. 45(13). DOI: 10.1177/0021998310382314

McGavin, R. L., T. Dakin, and J. Shanks. 2020. Mass-timber construction in Australia: Is CLT the only answer? *Bioresources.com* 15(3):4642–4645.

Neiderwestberg, J., J. Zhou, and Y. H. Chui. 2014. Influence of boundary conditions in modal testing on evaluated elastic properties of mass timber panels. *In:* World Conference on Timber Engineering, August 10–14, 2014, Quebec City, Canada; Curran Associates Inc., NY, USA. pp. 527–536.

Santoni, A., S. Schoenwald, B. V. Damme, and P. Fausti. 2017. Determination of the elastic and stiffness characteristics of cross-laminated timber plates from flexural wave velocity measurements. *J. Sound Vibration* 400:387–401.

Shirmohammadi, M., A. Faircloth, and A. Redman. 2020. Determining acoustic properties of Australian native hardwood species. *Eur. J. Wood Wood Prod*. 78:1161–1171.

Spromann, R., M. Zauer, and Wagenfuhr, A. 2017. Characterization of acoustic and mechanical properties of common tropical woods used in classical guitars. *Results Phys*. 7:1737–1742.

Steiger, R., D. Gulzow, and A. Gsell. 2010. Non-destructive evaluation of stiffness properties of cross-laminated solid wood panels. *In:* 11th World Conference on Timber Engineering, June 20–24, 2010, Terntino, Italy; Curran Associates Inc., NY, USA. pp. 433–440.

Zhang, L., A. Tiemann, T. Zhang, T. Gauthier, K. Hsu, M. Mahamid, P. K. Moniruzzaman, and D. Ozevin. 2021. Nondestructive assessment of cross-laminated timber using non-contact transverse vibration and ultrasonic testing. *Eur. J. Wood and Wood Prod*. 79(6):1–13.

Zhou, J., Y. H. Chui, M. Gong, and L. Hu. 2017. Comparative study on measurement of elastic constants of wood-based panels using modal testing: Choice of boundary conditions and calculation methods. *J. Wood Sci*. 63:523–538. DOI:10.1007/s10086-017-1645-0

Zhou, J., Y. H. Chui, J. Neiderwestberg, and M. Gong. 2020. Effective bending and shear stiffness of cross-laminated timber by modal testing: Method development and application. *Compos. Part B*. 198:108225. DOI:10.1016/j.compositesb.2020.108225